From ‘fixed dose combinations’ to ‘a dynamic dose combiner’: 3D printed bi-layer antihypertensive tablets.

Muzna Sadia[1], Abdullah Isreb[1], Ibrahim Abbadi[1], Mohammad Isreb[2], David Aziz[1], Amjad Selo[3], Peter Timmins[4], Mohamed A Alhnan[1]*

[1] School of Pharmacy and Biomedical Sciences, University of Central Lancashire, Preston, Lancashire, UK

[2]School of Pharmacy, University of Bradford, Richmond Road, Bradford, UK

[3]School of Pharmacy, University of Nottingham, Nottingham, UK

[4] Department of Pharmacy, University of Huddersfield, Huddersfield, UK

*Corresponding author: MAlbedAlhnan@uclan.ac.uk

University of Central Lancashire, MB025 Maudland Building, Preston PR1 2HE, UK

Tel: +44 (0)1772 893590, Fax: +44 (0)1772 892929

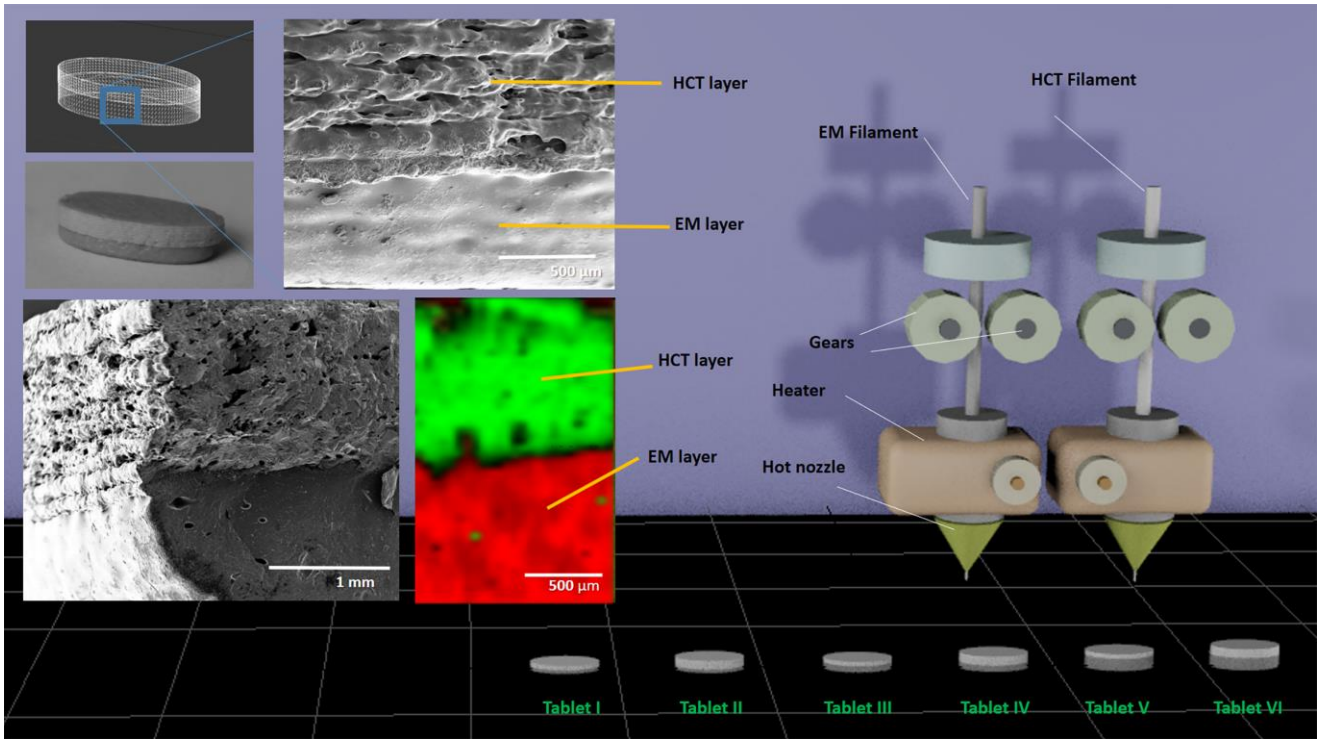
HCT layer
EM layer
500 µm
HCT layer
EM layer
1 mm
500 µm
HCT Filament
EM Filament
Gears
Heater
Hot nozzle
Tablet I
Tablet II
Tablet III
Tablet IV
Tablet V
Tablet VI

A B S T R A C T

There is an increased evidence for treating hypertension by a combination of two or more drugs. Increasing the number of daily intake of tablets has been reported to negatively affect the compliance by patients. Therefore, numerous fixed dose combinations (FDCs) have been introduced to the market. However, the inherent rigid nature of FDCs does not allow titration of the dose of each single component for individual patient needs. In this work, flexible dose combinations of two anti-hypertensive drugs in a single bilayer tablet with a range of doses were fabricated using dual fused deposition modelling (FDM) 3D printer. Enalapril maleate (EM) and hydrochlorothiazide (HCT) loaded filaments were produced *via* hot-melt extrusion (HME). Computer software was utilized to design sets of oval bi-layer tablet of individualised doses. Thermal analysis and x-ray diffractometer (XRD) indicated that HCT remained crystalline in the polymeric matrix whilst EM appeared to be in an amorphous form. The interaction between anionic EM and cationic methacrylate polymer may have contributed to a drop in the glass transition temperature (Tg) of the filament and obviated the need for a plasticiser. Across all tablet sets, the methacrylate polymeric matrix provided immediate drug release profiles. This dynamic dosing system maintained the advantages of FDCs while providing a superior flexibility of dosing range, hence offering an optimal clinical solution to hypertension therapy in a patient-centric healthcare service.

1. Introduction

The use of FDCs to enhance or simplify the treatment and to enhance patient compliance is a common approach in the management of long term conditions e.g. type 2 diabetes, HIV and hypertension (Bangalore et al., 2007; Desai et al., 2013). The history of combining multiple drugs in fixed doses dates back to 1950s, where the first combination was launched as combined antihypertensive treatment (Wofford, 1997). At present, hypertension is often treated using several multiple drug classes, that are clinically used as dual or triple combinations (Wan et al., 2014).

FDCs offer a myriad of benefits in treatment of hypertension; improving adherence (Castellano et al., 2014; Laurent et al., 2004) and reducing number of tablets intake. Hence, they facilitate a simplified streamlined schedule. Moreover, combining two or more therapeutics at lower doses can offer superior clinical output than single agent in maximal dose (Garber et al., 2003; Haak et al., 2012). In addition, FDCs can offer more cost-effective therapeutic option than monotherapy (Bell, 2013). For instance, FDCs has lower cost in comparison to individual drugs as the cost of manufacturing, packaging and distribution is lowered (Desai et al., 2013; Gupta and Ramachandran, 2016).

Although convenient, the system is often too rigid to accommodate to changing an individual patient's needs e.g. the dose titration is particularly challenging for FDCs in a clinical setup (Xu et al., 2012) . For instance, if the prescriber identified the necessity to adjust the dose of one component in the FDC, a commonly used solution is the replacement of FDC with two separate dosage forms. In general, the doses in FDCs are designed to cover general population and hence they are less capable to meet the needs of small number of patients (Sleight et al., 2006).

3D printing is an emerging platform that offers many benefits in case of medicines personalisation (Alhnan et al., 2016; Prasad and Smyth, 2016). For instance, a dosage form can be fabricated according to the individual patient's need with reduced number of steps involved in manufacturing while excluding the need of expensive designated facilities (Skowyra et al., 2015). Extrusion based 3D printing is capable of making a polypill with a distinct release profile (Khaled et al., 2015a, b). Although the technique offers the advantage of operation at room temperature, it often requires a long printing and drying time (typically 25 min and 24 h per tablet respectively)(Khaled et al., 2015a). It also mandates a significant compromise

between the viscosity of extruded materials, the size of the nozzle and the resolution of the finished product.

The low cost and widely used fused deposition modelling (FDM) 3D printers, however, offered a new and more accessible opportunity for on-demand fabrication of ready-to-use tablets/caplets, with flexible doses of drugs of extended release (Goyanes et al., 2014; Goyanes et al., 2015a; Pietrzak et al., 2015; Skowyra et al., 2015; Tagami et al., 2017) as well as immediate release profiles (Li et al., 2017b; Okwuosa et al., 2016; Sadia et al., 2016).

Although dual FDM 3D printing has been reported for multilayer or core-shell fabrication to achieve dual drug or enteric drug release (Goyanes et al., 2015c; Okwuosa et al., 2017), there has been no previous report for dose control in 3D printed combinations. This might be a reflection of the significant challenges often associated with dual FDM 3D printing; compatibility of the two materials, adhesion of printed layers in addition to the co-ordination of printing heads. These contributed to the difficulty of controlling drugs' doses in these multi-drug dosage forms.

Controlling the dose of 3D printed tablets might also raise a challenge in single head FDM 3D printing. Hot melt extrusion (HME) has been used to compound filaments as a feed for FDM 3D printing. Changing drug loading in such filaments, however, would significantly impact on the plasticity as well as drug release profiles. As FDM 3D printing process is particularly sensitive to changes in plasticity and rheological properties of the filament, it is hence of paramount importance to craft compatible filaments so the printer can fabricate structures of a similar release profile from wide range of doses.

In our previous work, we have reported a universal platform technology for 3D printing of immediate release tablets (Sadia et al., 2016). In this work, we provided an example of a dynamic dose regime for dual drug dosage forms for the treatment of hypertension. We highlighted some of major challenges of co-ordinating the printing of two different drug layers using dual FDM 3D printing and two model drugs of a high (enalapril maleate, EM) and a low miscibility (hydrochlorothiazide, HCT) with the matrix's polymer. The system's capacity to include a wide range of drug concentrations was also established.

2. Materials and methods

2.1.Materials

Tri-calcium phosphate (TCP), HCT and triethyl citrate (TEC) were purchased from Sigma-Aldrich (UK). Enalapril maleate (EM) was acquired from Kemprotec Ltd. (Cumbria, UK). Eudragit EPO was donated by Evonik Industries (Darmstadt, Germany).

2.2.Preparation and optimisation of filaments

For single HCT tablets, drug loaded filaments were compounded with increasing percentages of HCT (X) (i.e. X= 0 (blank), 2.5, 5, 7.5, 10, 12.5, 25 or 50% w/w). TCP (non-melting component) was employed as a substitute of HCT in each of the formulation to maintain incorporated solids content relative to the polymer. The final ratios of the formula were Eudragit EPO: TEC: HCT: TCP (46.75:3.25: X: 50-X), where X is the percentage of HCT in the filament (**Table 1**).

For bilayer tablets, two types of filaments were extruded containing either HCT or EM.

HCT filaments (25% HCT) were produced at ratio: Eudragit EPO: TEC: HCT: TCP (46.75:3.25: 25: 25% w/w) as described above. This HCT loading was selected in order to fabricate bi-layer tablets of relatively similar volumes of EM and HCT layers and contain clinically recommended doses of for both drugs.

In case of EM, two filaments with similar levels of plasticiser (TEC 3.25% and 2.5%) were initially produced using a 1.25 mm nozzle and ratios of EPO: TEC: EM: TCP 46.75:3.25:15:35 or 47.50:2.50:15: 35 respectively. However, these filaments were deemed too flexible and incompatible with FDM 3D printing process. Hence, a third filament with no plasticiser (without TEC) was produced at ratio EPO: EM: TCP 35:15:50 respectively (**Table 1**), where FDM 3D printing-compatible filament structure was restored through reducing polymer concertation and increasing the non-melting component (TCP).

All filaments were then extruded using a HAAKE MiniCTW hot melt extruder (Thermo Scientific, Karlsruhe, Germany) equipped with standard counter flow conical twin-screws of two stages conveying domains (22 cm) (**Supplementary data, Fig. S1**). The materials were accurately weighed (10 g), mixed in pestle and mortar for 5 min, and then manually fed and extruded at 100 °C and screw speed of 120 and 35 rpm for mixing and extrusion respectively. The average torque during mixing was about 5 Nm for both filaments.

With the drop of compression forces within the nozzle length, EM and HCT filaments showed different levels of expansion as they flew out of the nozzle head. To achieve a target diameter of the extruded filament of 1.7 mm, the difference in expansion level of the filaments was compensated by equipping the extruder with two different sizes of nozzle heads (1.25mm and 1 mm for HCT and EM respectively). The diameter for produced filaments was measured at 1.70± 0.01 and 1.71± 0.01 mm for HCT and EM respectively. The measurement were carried out using a Clarke CM145 electronic digital callipers (London, UK).

2.3.Design and 3D printing of tablets

Tablets were fabricated with HME based filaments using a dual FDM 3D printer, Makerbot Replicator 2X (Makerbot Industries, LLC, USA). The templates were designed using Autodesk® 3ds Max Design 2016 software version 18.0 (Autodesk, Inc., USA). The design was saved in a stereolithography (.stl) file format and was imported to the 3D printer's software, MakerWare Version 2.4.0.17 (Makerbot Industries, LLC, USA). Tablets were printed using modified settings of for PLA filament: as follows: type of printer: Replicator 2X; type of filament: PLA; resolution: standard; speed of extruding and traveling were 90 and 150 mm/s respectively; infill: 100% and a layer: height of 200 µm without supports or rafts. The temperatures for the nozzle and build plate of the 3D printer were 135 °C and 60 °C respectively.

Two sets of tablets were printed:

i) Single HCT tablets. In order to assess the release profile of the tablets of wide range of drug concentration, a series of tablet of identical dimensions (12 x 4.7 x 4.63 mm) has been printed for each HCT loading (2.5, 5, 7.5, 10, 12.5, 25 or 50%).

ii) HCT-EM Bi-layer. Six sets of bilayer tablets were fabricated with the combination of the following doses; HCT: EM 25:5, 25:10, 25:20, 12.5:5, 12.5:10 or 12.5: 20 mg:mg **(Table 2)**. The Lower layer (first layer to be printed) was fabricated using 15% EM filament while the upper layer was based on 25% HCT filament.

In order to achieve these doses, tablets of identical length and width (x=12 and y=6 mm) were designed while the height (z) was adjusted to allow the control of the printed volume of each layer and in turn its final mass and dose. The dose was calculated as:

$$D_1 = 0.25\ W_1 \text{ and } D_2 = 0.15\ W_2$$

where D_1 and D_2 are the individual doses of HCT and EM, and W_1 and W_2 are the weight of layer containing 25% HCT or 15% EM respectively.

The tablets were printed (n=4) and a linear curve was plotted between the theoretical volume and actual mass of the printed tablets.

$$W_1 = D_1/0.25 = 1.4275\ V_1 - 5.5707$$

$$W_2 = D_2/0.15 = 1.5682\ V_2 - 8.1756$$

Where V_1 and V_2 are the volume of the HCT and EM layer in the bi-layer tablet.

The final dimensions of the layers to achieve the target dose are shown in **Table 3**.

2.4.Thermal analysis

Samples (5 mg) of raw materials and filaments were placed in TA aluminium pans 40 µL (standard) and pin-holed lids and analysed using a differential scanning calorimeter (DSC) Q2000 (TA Instruments, Elstree, Hertfordshire, UK). Samples were heated at a rate of 10 °C/min, from -50 to 280 °C preceded by a 1 min isotherm at -50 °C. The analysis was carried out under a purge of nitrogen at 50 mL/min. The collected data were analysed using a TA Universal Analysis 2000 v 4.5A software (TA Instruments, Elstree, Hertfordshire, UK).

Thermal decomposition profiles were collected using a Thermogravimetric analyser TGA Q500 (TA Instruments, Hertfordshire, UK). Samples of raw materials and filaments (10 mg approx.) were placed in a 40 µL standard aluminium pan previously tared in a 100 µL sample platinum pan and were heated from 25 to 500 °C at a rate of 10 °C/min under nitrogen flow of 40 and 60 mL/min for balance and sample respectively.

In order to assess the impact of long term filament residence in hot nozzle during dual FDM 3D printing, drugs (as received) and filaments with HCT and EM at concentrations of 25% and 15% respectively were analysed by a thermo-scan from 25 to 140 °C with an isotherm of 30 min at the 3D printing temperature (135 °C). The changes in the mass of samples were then analysed using TA Universal Analysis 2000 v 4.5A software (TA Instruments, Elstree, Hertfordshire, UK).

2.5. X-ray diffractometer (XRD)

XRD analysis was carried out for raw materials, filaments and tablets using powder X-ray diffractometer, D2 Phaser with Lynxeye (Bruker, Germany). A scan was run from $2\theta = 7°$ to

50° with 0.1° step width and a 1s time count over 60 min. The divergence and scatter slits were 1mm and 0.6mm respectively. The X-ray wavelength was 0.154 nm using a Cu source, the voltage of 30kV and filament emission of 10 mA.

2.6.FT-IR Spectra measurements

FT-IR measurement for raw materials, filaments and tablets was carried out using Nicolet 5700 FT-IR spectrophotometer (Thermo Nicolet, Waltham, USA). The spectra were scanned between 4000 and 500 cm^{-1} at a resolution of 2 cm^{-1} using 128 accumulations/scan.

2.7. *Solubility parameter*

Hansen solubility parameters for the polymer and the drugs were calculated using HSPiP (version 5.0.08) software. Eudragit EPO was calculated by splitting its structure to its 3 parts: butyl methacrylate, (2-dimethylaminoethyl) methacrylate, methyl methacrylate and calculating the solubility parameters of a blend of the three parts in a ratio of 1:2:1 (ref Handbook of pharmaceutical excipients 7^{th} edition). Enalapril maleate was also calculated as a blend ratio of 3.2:1 of Enalapril and Maleate (molecular weight ratio).

2.8.Rheology studies

An Anton Paar Shear Rheometry Physica MCR 302 (Graz, Austria) with 25 mm parallel plates was employed using a 0.5mm gap distance in oscillation mode. Linear viscoelastic region (LVR) was studied with 1% strain amplitude. Samples were measured using an amplitude sweep at an angular frequency range from 100 to 0.01 rad/sec and angular frequency of 10 rad/sec. Temperature was set as two cycles scan at 135°C (the temperature of FDM 3D printing) and readings were collected every 5 sec.

2.9.Characterisation of filament and tablets

The mechanical properties of bilayer tablets were assessed using Erweka TAR 10 friability tester (Erweka GmbH, Heusenstamm, Germany), 10 tablets were randomly selected, weighed and placed in a friability tester and the drum was then rotated at 25 rpm for 4 min. To evaluate the hardness of the 3D printed bilayer tablets, an Agilent 200 Tablet Hardness tester equipped with a standard jaw plate (Agilent Technologies, Germany) was employed

To analyse the impact of high temperature on drug after HME and 3D Printing, the tablets were assessed for drug content. Tablets (n=3) were randomly selected from each set and weighed. Each tablet was then placed in 1000 mL volumetric flask containing 0.1 M HCl and sonicated

for 2 h. The solutions were then filtered using 0.22 µm Millex-GP syringe filters (Merck Millipore, USA) in a 1 mL vial. Simultaneous quantification was then carried out using an Agilent UV-HPLC 1260 series (Agilent Technologies, Inc., Germany) equipped with Kinetex C18 column (100 × 2.1 mm, particle size 2.6 mm) (Phenomenex, Torrance, USA). The mobile phase was acetonitrile: water (adjusted to pH 3 with o-phosphoric acid) and was measured at 230 nm. A gradient method was used for the quantification of drugs in HPLC (Water pH 3: acetonitrile 95:5 for 0-3 min, 95:50 to 50:50 from 3 to 8 min, 95:5 from 8.01 to 14 min) with a stop time of 14 min. The injection volume was 20 µL and the column temperature was set at 25 °C. The retention time for HCT and enalapril was 9.6 and 10.14 min respectively. The details of the method validation are available in **Supplementary data Table S1 and Fig. S2.**

In order to detect the level of EM impurities in filament and tablet, EM filament and tablets (n=3) were dissolved as described above and the resultant solutions were analysed using adapted HPLC method from British Pharmacopeia (Commission, 2018). The above-mentioned HPLC system was equipped with a C8-EPS column (5 µm, 250 × 4.6 mm) (Hichrom Dr Maisch GmbH, Germany). The mobile phase was 25:75 acetonitrile: water (1.38 g/L NaH_2PO_4 pH adjusted to 2.2 with orthophosphoric acid) and was measured at 215 nm. The flow rate was 1.5 mL/min, the injection volume was 50 µL, the stop time was 4 min and the column temperature was 20 °C. The relative retentions with reference to enalapril (retention time ~2.2 min) are: 0.4 for impurity C (Enalaprilat) and 1.5 for impurity D (Diketopiperazine).

2.10. Scanning electron microscopy (SEM) and Raman spectroscopy

The surface morphology of FDM 3D printed of bilayer tablets was assessed using JCM-6000 Plus Neoscope benchtop SEM (JEOL ltd. Japan). Samples were placed on metallic stubs and gold coated under vacuum for 2 min using JFC-1200 Fine Coater (Jeol, Tokyo, Japan), prior to imaging. Raman data of the raw material and mapping spectra of the side of the 3D printed tablet were collected on a Renishaw Raman microscope (Renishaw PLC, Gloucestershire, UK) using Wire version 1.3 software. The spectra were obtained by exciting the sample with a laser line at 785 nm. The samples were viewed and Raman data collected through a 5X objective. The spectra were acquired for 10 sec per stage position resulting in total acquisition time of about 32 hours.

2.11. In vitro drug release from 3D printed tablets

In vitro drug release study was carried out using USP II Erweka DT600 dissolution tester (Erweka GmbH, Heusenstamm, Germany). For dissolution tests, tablets (n=3) from each of the

sets: HCT: EM 5:12.5, 10:25 and 20:25 mg were placed in dissolution vessels containing 900 mL of 0.1M HCl. The paddle speed was set to 50 rpm while the temperature was maintained at 37 °C. The samples (4 mL) were collected at 5, 10, 15, 20, 25, 30, 40, 50 and 60 min using Luer-Lock syringes of 5 mL capacity. The samples were then filtered out in 2 mL HPLC vial through Millex-HA 0.45 µm filters. The medium was then replenished with 4 mL of 0.1M HCl kept at same temperature. The quantitative analysis was then carried out using the HPLC protocol specified above. All dissolution experiments were carried out under sink conditions for both model drugs. (Budavari et al., 1996; Yalkowsky and R.M., 1992).

3. Results and discussion

The proposed dynamic dose dispenser is based on dual 3D printer head, each nozzle is loaded with individual loaded filament and dose is controlled by varying the thickness of each layer in the tablet (**Fig. 1**). To achieve this, a universal filament system for immediate release (Sadia et al., 2016) was adapted to include two antihypertensive drugs: EM and HCT. Firstly, the flexibility of the method to comprise different concentration of HCT has been investigated by varying drug concentration from 2.5% to 50% w/w.

TGA studies showed no significant weight loss within the range of HME and 3D printing temperatures for all HCT filaments (**Fig. 2A**). However, increasing the temperature >220 ^{o}C led to a two-step degradation at approximately 310 and 420 ^{o}C. HCT was reported to degrade above 300 ^{o}C in a multi-stage reaction (Menon et al., 2002). Decreasing HCT ratio in the filament led to lower degradation percentage at elevated temperature (>400^{o}C), this was expected as filaments of low HCT concentrations contained a significant amount of thermally stable filler (TCP). DSC thermographs showed a Tg range of 22.9-35°C across all ratios of HCT (**Fig. 1B**). This suggests that the drug had a limited plasticising impact on filaments. The yielded filaments were compatible with FDM 3D printing process. Eudragit EPO degrades >250 ^{o}C and thermal signals of the degradation might interfere with the melting point of HCT (T_m= 267 ^{o}C), therefore, it was not possible to confirm the presence of HCT melting point in the thermograph of these filaments.

XRD analysis were used to confirm the physical form of HCT in the filament **(Fig. 3)**, the diffraction peaks of HCT (as received) at 2θ = 16.65°, 19.13°, 20.95° and 24.64° were typical for HCT crystals (Khaled et al., 2015a). The presence of intensity peak at 2θ = 19.13^{o} in all HCT filaments indicated that HCT remained in crystalline form after undergoing through the thermal processing of HME**.** The use of TCP as a complimentary filler to replace HCT allowed

the production of filament of consistent properties. *In vitro* release drug from identical size tablets showed no significant difference of percentage of drug release at T=30 min (p>0.05) **(Fig. 4)**. All tablets were compatible with USP monograph for the dissolution of HCT tablets (USP, 2007). This is of particular importance as it provides an alternative to controlling the dose of the 3D printed tablet by changing the size of the tablet, as previous reports indicated that surface area have a directly impact on its release pattern (Goyanes et al., 2015b; Pietrzak et al., 2015; Skowyra et al., 2015).

TGA of EM (as received) showed low weight loss within the operational temperature of HME and 3D printing processes (100 and 135 °C) (**Fig. 5A**). EM loaded filaments demonstrated a small level of weight loss (up to 3%) across the different ratios of plasticiser. EM loaded filaments were initially produced using similar plasticiser concentrations of that used with HCT (TEC 2.5% and 3.25% w/w) and yielded filaments of T_g values <15 °C (**Fig. 5B**). This rendered the filament excessively flexible to be compatible with the FDM 3D printing procedure. Highly flexible filament is prone to frequent bending and deformation within gears that feed the hot nozzle of the FDM 3D printer. Since the drop in the Tg suggests that EM had a plasticising effect on the methacrylic polymer, a new formulation was adapted by the removal of plasticiser (0 % TEC). By relying on drug's plasticizing capacity, the resultant filament showed a T_g of 50 ^{o}C (**Fig. 5B**), the latter proved more suitable for FDM 3D printing process.

On the other hand, the absence of melting peak of EM at 145 ^{o}C suggested that EM was in amorphous state within both the filament and the tablet. This suggest that amorphous form integrity of EM were maintained following the 3D printing process. XRD patterns of EM (as received) showed intensity peaks at 2θ = 5.2°, 10.41° and 20.65°, which are distinguished diffraction peaks of EM crystals (Kiang et al., 2003). These peaks were absent in the filaments hence confirmed that the EM was in amorphous form within EM filament. The high level of miscibility of Eudragit EPO and EM might be related to the opposite charge of the anionic malate and the cationic polymer chains.

FTIR spectrum for Eudragit EPO showed bands at 2770 and 2822 cm^{-1} corresponding to the absorption band of non-protonated dimethylamine of the polymer (**Supplementary data Fig. S3**), the filament showed a depression in these bands and hence suggest that EM neutralized the polymer. FTIR spectrum EM showed a band at 1750 cm^{-1} can be observed in both drug and physical mixture but disappeared in the filament and tablets. The band at 1750 cm^{-1} represents the stretching of C=O group (Ip and Brenner, 1987). The disappearance of this in the filament

and tablets might indicate the carboxylic group of EM has interacted with the amino group of Eudragit EPO. These data indicate the cationic amino groups of Eudragit EPO and the carboxylic group of maleate (Ramirez-Rigo et al., 2014; Wang et al., 2004). Such interaction between Eudragit EPO and anionic molecules (EM) in HME based product has also been reported in solid complexes prepared using solvent evaporation methods (Quinteros et al., 2011; Ramirez-Rigo et al., 2014).

The miscibility of the two model drugs with Eudragit EPO can be predicted by Hansen solubility parameter (HSP). The differences in HSP values between Eudragit EPO on one hand and EM and HCT on the other hand are $\Delta\delta$= 1 and 17.7 $MPa^{1/2}$ respectively (**Table 4**). Therefore, it is expected that EM to be miscible and form a homogeneous mixture with Eudragit ($\Delta\delta < 7$ $MPa^{1/2}$), while HCT crystals ($\Delta\delta > 7$ $MPa^{1/2}$) are likely to remain suspended within the polymethacrylate matrix.

Rheological studies showed that the complex viscosity of Eudragit EPO was ~8750 Pa.sec at the FDM 3D printing temperature (**Fig 6A, Supplementary data Figs. S4 and S5**). Upon compounding into filament via HME, the complex viscosity was dropped to approximately 4000 Pa.sec at 1 rad/sec angular frequency (HTC 0%). This drop in viscosity could be linked to the reduced T_g in these filaments (with the addition of plasticiser) and the decreased polymeric chains interaction (**Fig 6A**). Our research group previously reported that the introduction of a non-melting filler (TCP) to enhance the viscoelastic behaviour in the system (Sadia et al., 2016). In current research, replacing a non-melting filler (TCP) with equivalent amount of low miscibility drug, HTC at wide range of percentages (2.5-50%) resulted in comparable rheological behaviours with a predominantly viscous character with G`<G`` **(Supplementary data Fig. S4)**. However, when a drug with high miscibility with the polymer (EM) is incorporated in the filament, the complex viscosity dropped significantly (~743 Pa.sec at 1rad/sec angular frequency) (**Fig 6B**). This illustrates the importance of drug miscibility with the polymer on the rheological performance of the filament in FDM 3D printing.

In dual FDM 3D printing, two thermal nozzles are orchestrated to extrude the filament in alternative fashion to fabricate multi-material structures. Hence while one filament is being processed through the nozzle, the other is held at elevated temperature in the second nozzle. Therefore, a retraction function has been introduced to many dual printing software to mitigate this effect. It is therefore important to assess the thermal stability of the filament at the printing temperature (135ºC) for a prolonged time. Both filaments were subjected to a 30-min isotherm

at 135°C to analyse the impact of prolonged thermal exposure on weight loss. The data showed that HCT revealed no significant weight loss throughout the thermal holding period whilst HCT filament showed a minimal weight loss of <1% (**Fig. 7 A1, A2)**. However, EM (as received) suffered approximately 20% weight loss under the same thermal test. The weight loss in the EM loaded filament (1.9%) can be attributed to EM degradation **(Fig. 7 B1,B2)**. Hence, the lower layer in the bi-layer structure of the tablet (which was printed first) was chosen to contain EM in order to minimise the period of exposure of EM to an elevated temperature of the printing process. In dual 3D printing, retraction of 'stand-by' head prevents the long exposure of the materials to elevated temperature. When this approach was applied in bilayer tablets, no traces of impurities C or D for EM was detectable by HPLC. We have also noted that the temperature of both heads is elevated to its target regardless of the order of the printing. It might be of useful to delay the onset of heating of the stand-by nozzle to minimise degradation. However, this needs to be balanced with minimizing lag time between printing layers as well as nozzle blockage.

Six sets of bilayer tablets with distinctive dose of EM and HCT were printed. The drug contents of each layer were controlled by variating the thickness of individual drug layer within the structure **(Fig. 1 A).** Drug contents study was carried out in the filaments containing 25% HCT and 15% EM followed by 3D printed bilayer tablets **(Table 2)**. The target doses were achieved for the majority of the tablet sets, however, increased deviation was noted particularly in low strength tablets (deviation was 11.35 % of the target dose in Tablet I design). The variation of content and weight uniformity could be mitigated by improving the consistency of the mixing and applying a tight control on the filament diameter.

The yielded tablets showed excellent mechanical properties with no weight loss following the friability test. This might be a result of their polymer-rich structure and provides an important advantage for providing an easy-to-handle dosage form that is readily available without the delay of finishing or drying process of other 3D printing technologies. When the crushing strength of 3D printed bi-layer tablets were tested, the tablets showed a minor deformation at strength >135N without any crack propagation. These results conform to previous reports on tablets produced by FDM 3D printing (Goyanes et al., 2014; Goyanes et al., 2015c). While our examples are confined to the recommended doses of the two model drugs in the treatment of hypertension. Such a system can be adapted for elaborative range of intermediate doses, this can be particularly relevant to drug where doses are often calculated per body weight.

The design of the bilayer tablets and an image of an exemplar tablet are shown in **Figs. 8A, B**, SEM images indicated that both drug layers were composed of 200 μm layer (**Figs. 8C, D**). It is interesting to highlight that HCT layer in the tablet was dominated with visible pores and embedded particles, while EM layers had a smoother surface and were more fused. On the other hand, Raman imaging indicated the consistent distribution of the drugs within each layer (**Fig. 8E**).

Our previous investigation indicated that the Eudragit EPO based tablets tend to erode within the first 15 min of disintegration test rather than disintegration into granules or particles (Sadia et al., 2016). This is directly related to the polymer-rich matrix structure of the tablet. Recently, the use of perforating channels within tablet design have been reported to accelerate tablets disintegration and dissolution (Sadia et al., 2017).

The two model drugs were reported to have different aqueous solubility [722mg/L (Yalkowsky and R.M., 1992) and 25 000 mg/L (Budavari et al., 1996) for HCT and EM respectively]. Nevertheless, the *in vitro* drug release patterns from three sets of bilayer tablets showed similar release patterns (**Fig. 9)**. It is worth noting that this was achieved despite the difference in the physical form of the two model drugs within the polymeric matrix (amorphous EM and crystalline HCT). This suggests that drug release is principally governed by the erosion of methacrylate polymeric matrix (Li et al., 2017a). The cationic polymer ionises and dissolves upon tablet introduction to gastric medium (Dierickx et al., 2012; Onoue et al., 2012) hence allowing both drugs to be released at similar rates. Such approach should be balanced with risk of slowing drug release, as polymer erosion might become the rate-limiting step when larger dosage forms are employed. In fact, the release of EM was slightly slowed down when higher doses where applied. This might be attributed to the loss of surface-to-mass ratio of thicker layers.

The versatility of this dosing system is of particular advantage in practice, when the dose of one or both drugs in the bilayer tablet are sought to be modified without changing the dose of the other drug. Patients who need secondary prevention post myocardial infarction, for instance, may need to increase their ACE inhibitor while ensuring that the diuretic dose is kept constant (National Clinical Guideline Centre, 2013). (Centre, 2013)

In summary, we have reported the fabrication of bilayer tablets to achieve a new option of hypertensive patients (dose combination with dynamic dosing system). In a future scenario, physicians will be able to modify the dose for instance in response to patient's clinical data

while maintaining a single dose and without the need to change direction to the patient or request tablet splitting.

4. Conclusion

We demonstrated the use of dual 3D printing to achieve a dynamic dose dispensing. This dispensing system holds the advantages of fixed dosage combinations while offering a flexibility on dosing in a drug combination, hence ensuring that patient's individual needs are continuously fulfilled. Despite differences in model drug miscibility in the polymer base, FDM 3D-printing-compatible filaments were engineered *via* the manipulation of plasticiser level and the addition of inert non-melting component. The use of methacrylate based bi-layer tablet system offers covering a wide range of drug loading (within the filament). Each tablet was printed with dual drugs and distinct dose combinations. Although further refinement steps are needed to improve the weight and dose consistency of this flexible dosing system, the system holds a clinical potential for providing bespoke solutions to hypertensive patients.

Acknowledgments

The authors would like to thank UCLAN Innovation Team for this support and Mrs Rim Arafat for her help with graphics design. The authors would also like to acknowledge the School of Medicine and Biomedical Sciences, Sheffield University for their support with μCT data.

Conflicts of interest M A Alhnan is the innovator in pending patent applications WO 2016038356 A1, P1607548.3 GB and GB 1519128.1 in the field of 3D printing of medicines.

List of Figures

Fig. 1. (A) Rendered images (Autodesk 3DS Max) of bi-layered designs with unique dosage combination of EM and HCT, **(B)** Schematic diagram of dual 3D printer with EM and HCT loaded filament deployed in individual nozzles. The tablet were composed of lower EM layer and an upper HCT layer of variable volume to achieve different doses.

Fig. 2. (A)TGA thermal degradation profiles and **(b)** DSC thermographs of HCT loaded filament with HCT 0,2.5, 5, 7.5, 10, 12.5, 25 or 50%, of Eudragit EPO, HCT and (C) DSC thermographs of Eudragit EPO, HCT and drug loaded filament.

Fig. 3. XRD patterns of HCT loaded filament with HCT 0,2.5, 5, 7.5, 10, 12.5, 25 or 50%,

Fig. 4. *In vitro* release pattern of 3D printed tablets produced from HCT filament with HCT loading of 0,2.5, 5, 7.5, 10, 12.5, 25 or 50%,

Fig. 5. A) TGA thermal degradation profiles, **(b)** DSC thermographs and **(C)** XRD patterns of EM and EM loaded filament with different levels of plasticiser (TEC 0, 2.5, 3.25%).

List of Tables

Supplementary data

References

Alhnan, M.A., Okwuosa, T.C., Sadia, M., Wan, K.W., Ahmed, W., Arafat, B., 2016. Emergence of 3D Printed Dosage Forms: Opportunities and Challenges. Pharm Res 33, 1817-1832.

Bangalore, S., Kamalakkannan, G., Parkar, S., Messerli, F.H., 2007. Fixed-dose combinations improve medication compliance: a meta-analysis. Am J Med 120, 713-719.

Bell, D.S., 2013. Combine and conquer: advantages and disadvantages of fixed-dose combination therapy. Diabetes Obes Metab 15, 291-300.

Budavari, S., O'Neil, M., Smith, A., Heckelman, P., Obenchain, J., 1996. The Merck Index, 12th ed., Entry# 3605.

Castellano, J.M., Sanz, G., Penalvo, J.L., Bansilal, S., Fernandez-Ortiz, A., Alvarez, L., Guzman, L., Linares, J.C., Garcia, F., D'Aniello, F., Arnaiz, J.A., Varea, S., Martinez, F., Lorenzatti, A., Imaz, I., Sanchez-Gomez, L.M., Roncaglioni, M.C., Baviera, M., Smith, S.C., Jr., Taubert, K., Pocock, S., Brotons, C., Farkouh, M.E., Fuster, V., 2014. A polypill strategy to improve adherence: results from the FOCUS project. J Am Coll Cardiol 64, 2071-2082.

Centre, N.C.G., 2013. MI - secondary prevention, Partial update of NICE CG48 Methods, evidence and recommendations, available online: https://www.nice.org.uk/guidance/cg172/evidence/myocardial-infarction-secondary-prevention-full-guideline-pdf-248682925 (last accessed 30/9/2017).

Commission, B., 2018. British pharmacopoeia. The Stationary Office, London.

Desai, D., Wang, J., Wen, H., Li, X., Timmins, P., 2013. Formulation design, challenges, and development considerations for fixed dose combination (FDC) of oral solid dosage forms. Pharm Dev Technol 18, 1265-1276.

Dierickx, L., Saerens, L., Almeida, A., De Beer, T., Remon, J.P., Vervaet, C., 2012. Co-extrusion as manufacturing technique for fixed-dose combination mini-matrices. Eur J Pharm Biopharm 81, 683-689.

Garber, A.J., Donovan, D.S., Jr., Dandona, P., Bruce, S., Park, J.S., 2003. Efficacy of glyburide/metformin tablets compared with initial monotherapy in type 2 diabetes. J Clin Endocrinol Metab 88, 3598-3604.

Goyanes, A., Buanz, A.B., Basit, A.W., Gaisford, S., 2014. Fused-filament 3D printing (3DP) for fabrication of tablets. Int J Pharm 476, 88-92.

Goyanes, A., Buanz, A.B., Hatton, G.B., Gaisford, S., Basit, A.W., 2015a. 3D printing of modified-release aminosalicylate (4-ASA and 5-ASA) tablets. Eur J Pharm Biopharm 89, 157-162.

Goyanes, A., Robles Martinez, P., Buanz, A., Basit, A.W., Gaisford, S., 2015b. Effect of geometry on drug release from 3D printed tablets. Int J Pharm 494, 657-663.

Goyanes, A., Wang, J., Buanz, A., Martinez-Pacheco, R., Telford, R., Gaisford, S., Basit, A.W., 2015c. 3D Printing of Medicines: Engineering Novel Oral Devices with Unique Design and Drug Release Characteristics. Mol Pharm 12, 4077-4084.

Gupta, Y.K., Ramachandran, S.S., 2016. Fixed dose drug combinations: Issues and challenges in India. Indian J Pharmacol 48, 347-349.

Haak, T., Meinicke, T., Jones, R., Weber, S., von Eynatten, M., Woerle, H.J., 2012. Initial combination of linagliptin and metformin improves glycaemic control in type 2 diabetes: a randomized, double-blind, placebo-controlled study. Diabetes Obes Metab 14, 565-574.

Ip, D.P., Brenner, G.S., 1987. Enalapril Maleate. Analytical Profiles of Drug Substances 16, 207-243.

Khaled, S.A., Burley, J.C., Alexander, M.R., Yang, J., Roberts, C.J., 2015a. 3D printing of five-in-one dose combination polypill with defined immediate and sustained release profiles. J Control Release 217, 308-314.

Khaled, S.A., Burley, J.C., Alexander, M.R., Yang, J., Roberts, C.J., 2015b. 3D printing of tablets containing multiple drugs with defined release profiles. Int J Pharm 494, 643-650.

Kiang, Y.H., Huq, A., Stephens, P.W., Xu, W., 2003. Structure determination of enalapril maleate form II from high-resolution X-ray powder diffraction data. J Pharm Sci 92, 1844-1853.

Laurent, C., Kouanfack, C., Koulla-Shiro, S., Nkoue, N., Bourgeois, A., Calmy, A., Lactuock, B., Nzeusseu, V., Mougnutou, R., Peytavin, G., Liegeois, F., Nerrienet, E., Tardy, M., Peeters, M., Andrieux-Meyer, I., Zekeng, L., Kazatchkine, M., Mpoudi-Ngole, E., Delaporte, E., 2004. Effectiveness and safety of a generic fixed-dose combination of nevirapine, stavudine, and lamivudine in HIV-1-infected adults in Cameroon: open-label multicentre trial. Lancet 364, 29-34.
Li, J., Wang, X., Li, C., Fan, N., Wang, J., He, Z., Sun, J., 2017a. Viewing Molecular and Interface Interactions of Curcumin Amorphous Solid Dispersions for Comprehending Dissolution Mechanisms. Mol Pharm 14, 2781-2792.
Li, Q., Wen, H., Jia, D., Guan, X., Pan, H., Yang, Y., Yu, S., Zhu, Z., Xiang, R., Pan, W., 2017b. Preparation and investigation of controlled-release glipizide novel oral device with three-dimensional printing. Int J Pharm 525, 5-11.
Menon, D., El-Ries, M., Alexander, K.S., Riga, A., Dollimore, D., 2002. A thermal analysis study of the decomposition of hydrochlorothiazide. Instrum Sci Technol 30, 329-340.
Okwuosa, T.C., Pereira, B.C., Arafat, B., Cieszynska, M., Isreb, A., Alhnan, M.A., 2017. Fabricating a Shell-Core Delayed Release Tablet Using Dual FDM 3D Printing for Patient-Centred Therapy. Pharm Res 34, 427-437.
Okwuosa, T.C., Stefaniak, D., Arafat, B., Isreb, A., Wan, K.W., Alhnan, M.A., 2016. A Lower Temperature FDM 3D Printing for the Manufacture of Patient-Specific Immediate Release Tablets. Pharm Res 33, 2704-2712.
Onoue, S., Kojo, Y., Aoki, Y., Kawabata, Y., Yamauchi, Y., Yamada, S., 2012. Physicochemical and pharmacokinetic characterization of amorphous solid dispersion of tranilast with enhanced solubility in gastric fluid and improved oral bioavailability. Drug Metab Pharmacokinet 27, 379-387.
Pietrzak, K., Isreb, A., Alhnan, M.A., 2015. A flexible-dose dispenser for immediate and extended release 3D printed tablets. Eur J Pharm Biopharm 96, 380-387.
Prasad, L.K., Smyth, H., 2016. 3D Printing technologies for drug delivery: a review. Drug Dev Ind Pharm 42, 1019-1031.
Quinteros, D.A., Manzo, R.H., Allemandi, D.A., 2011. Interaction Between Eudragit (R) R E100 and Anionic Drugs: Addition of Anionic Polyelectrolytes and Their Influence on Drug Release Performance. J Pharm Sci 100, 4664-4673.
Ramirez-Rigo, M.V., Olivera, M.E., Rubio, M., Manzo, R.H., 2014. Enhanced intestinal permeability and oral bioavailability of enalapril maleate upon complexation with the cationic polymethacrylate Eudragit E100. Eur J Pharm Sci 55, 1-11.
Sadia, M., Arafat, B., Ahmed, W., Forbes, R.T., Alhnan, M.A., 2017. Channelled tablets: An innovative approach to accelerating drug release from 3D printed tablets. J Control Release 269, 355-363.
Sadia, M., Sosnicka, A., Arafat, B., Isreb, A., Ahmed, W., Kelarakis, A., Alhnan, M.A., 2016. Adaptation of pharmaceutical excipients to FDM 3D printing for the fabrication of patient-tailored immediate release tablets. Int J Pharm 513, 659-668.
Skowyra, J., Pietrzak, K., Alhnan, M.A., 2015. Fabrication of extended-release patient-tailored prednisolone tablets via fused deposition modelling (FDM) 3D printing. Eur J Pharm Sci 68, 11-17.
Sleight, P., Pouleur, H., Zannad, F., 2006. Benefits, challenges, and registerability of the polypill. Eur Heart J 27, 1651-1656.
Tagami, T., Fukushige, K., Ogawa, E., Hayashi, N., Ozeki, T., 2017. 3D Printing Factors Important for the Fabrication of Polyvinylalcohol Filament-Based Tablets. Biol Pharm Bull 40, 357-364.
USP, 2007. The United States Pharmacopeia: USP30. United States Pharmacopeial Convention Inc., Rockville, MD.
Wan, X., Ma, P., Zhang, X., 2014. A promising choice in hypertension treatment: Fixed-dose combinations. AJPS 9, 1-7.
Wang, S.L., Lin, S.Y., Chen, T.F., Cheng, W.T., 2004. Eudragit E accelerated the diketopiperazine formation of enalapril maleate determined by thermal FTIR microspectroscopic technique. Pharm Res 21, 2127-2132.

Wofford, J.L., 1997. History of fixed-dose combination therapy for hypertension. Arch Intern Med 157, 1044-1044.
Xu, X.S., Yuan, M., Nandy, P., 2012. Analysis of dose-response in flexible dose titration clinical studies. Pharm Stat 11, 280-286.
Yalkowsky, S.H., R.M., D., 1992. Aquasol Database of Aqueous Solubility, College of Pharmacy, University of Arizona, Tucson, AZ

Table 1 Composition and apparent density of drug loaded filaments

Filament	HCT	EM	TCP	Eudragit PO	TEC
HCT (0%)	-	-	50	46.75	3.25
HCT (2.5%)	2.5	-	47.5	46.75	3.25
HCT (5%)	5	-	45	46.75	3.25
HCT (7.5%)	7.5	-	42.5	46.75	3.25
HCT (10%)	10	-	40	46.75	3.25
HCT (12.5%)	12.5	-	37.5	46.75	3.25
HCT (25%)	25	-	25	46.75	3.25
HCT (50%)	50	-	-	46.75	3.25
EM (TEC 3.25%)*	-	15	35	46.75	3.25
EM (TEC 2.5%)*	-	15	35	47.50	2.5
EM (No TEC)	-	15	50	35	-

*Filaments were incompatible with FDM 3D printing

Table 2 Layer dimensions, filaments contents (loaded with HCT 25% or EM 15% w/w), target and achieved doses and dose efficiency of 3D printed tablets.

	Drug	Target dose (mg)	Bilayer tablet weight (mg) (Average ±SD)	SD%	Layer dimensions (X x Y x Z) (mm)	Filament content (%) ± SD	Achieved dose (mg) AV± SD
Bilayer Table I	EM layer	5	92±5.3	5.7%	12 x6 x 0.6	94.42±0.56	4.93±0.56
	HCT layer	12.5			12 x6 x 0.8	92.35±2.45	11.73±0.36
Bilayer Table II	EM layer	5	162.2± 2.9	1.8%	12 x 6 x 0.6	89.69±9.15	5.66±0.15
	HCT layer	25			12 x 6 x 1.6	91.98±2.73	25.82±0.68
Bilayer Table III	EM layer	10	124.6±4.4	3.5%	12 x 6 x 1.1	89.69±9.15	9.76±0.57
	HCT layer	12.5			12 x 6 x 0.8	91.98±2.73	12.95±1.07
Bilayer Table IV	EM layer	10	188.5±6.9	3.7%	12 x 6 x 1.1	89.69±9.15	9.64±0.13
	HCT layer	25			12 x 6 x 1.6	91.98±2.73	24.17±0.96
Bilayer Table V	EM layer	20	206.6±14.5	7%	12 x 6 x 2.2	96.98±1.39	20.11±0.64
	HCT layer	12.5			12 x 6 x 0.8	95.12±5.09	12.33±0.28
Bilayer Table VI	EM layer	20	266.9±7.4	2.8%	12 x 6 x 2.2	96.98±1.39	19.30±1.56
	HCT layer	25			12 x 6 x 1.6	95.12±5.09	24.85±3.03

Table 3 Dimensions, volume and expected mass and dose of the HCT and EM layers in bi-layer tablets.

Dose	Dimensions			Volume (mm^3)	Expected weight (mg)	Expected dose EM (mg)	Expected dose HCT (mg)
	X (mm)	Y (mm)	Z (mm)				
Dose 1	12	6	1.6	90.5	112	-	24.6
Dose 2	12	6	0.8	45.24	55.93	-	12.5
Dose 1	12	6	0.6	33.9	41.9	5.53	-
Dose 2	12	6	1.1	62.2	76.9	10.2	-
Dose 3	12	6	2.2	124	154	20.3	-

Table 4 Solubility parameter and its components of model drugs (HCT and EM) and Eudragit EPO in $MPa^{1/2}$

Compound	**δD**	**δP**	**δH**	**HSP**	**Δδ**
Eudragit EPO	16.8	5.6	6.0	18.7	-
EM	16.2	8.5	7.3	19.7	1
HCT	21.5	26.0	14.4	36.4	17.7

Where δD, δP and δH are the dispersion, polar, and hydrogen components of solubility parameter, (HSP) Hansen solubility parameter, and Δδ is difference in HSP of Eudragit EPO and model drug.

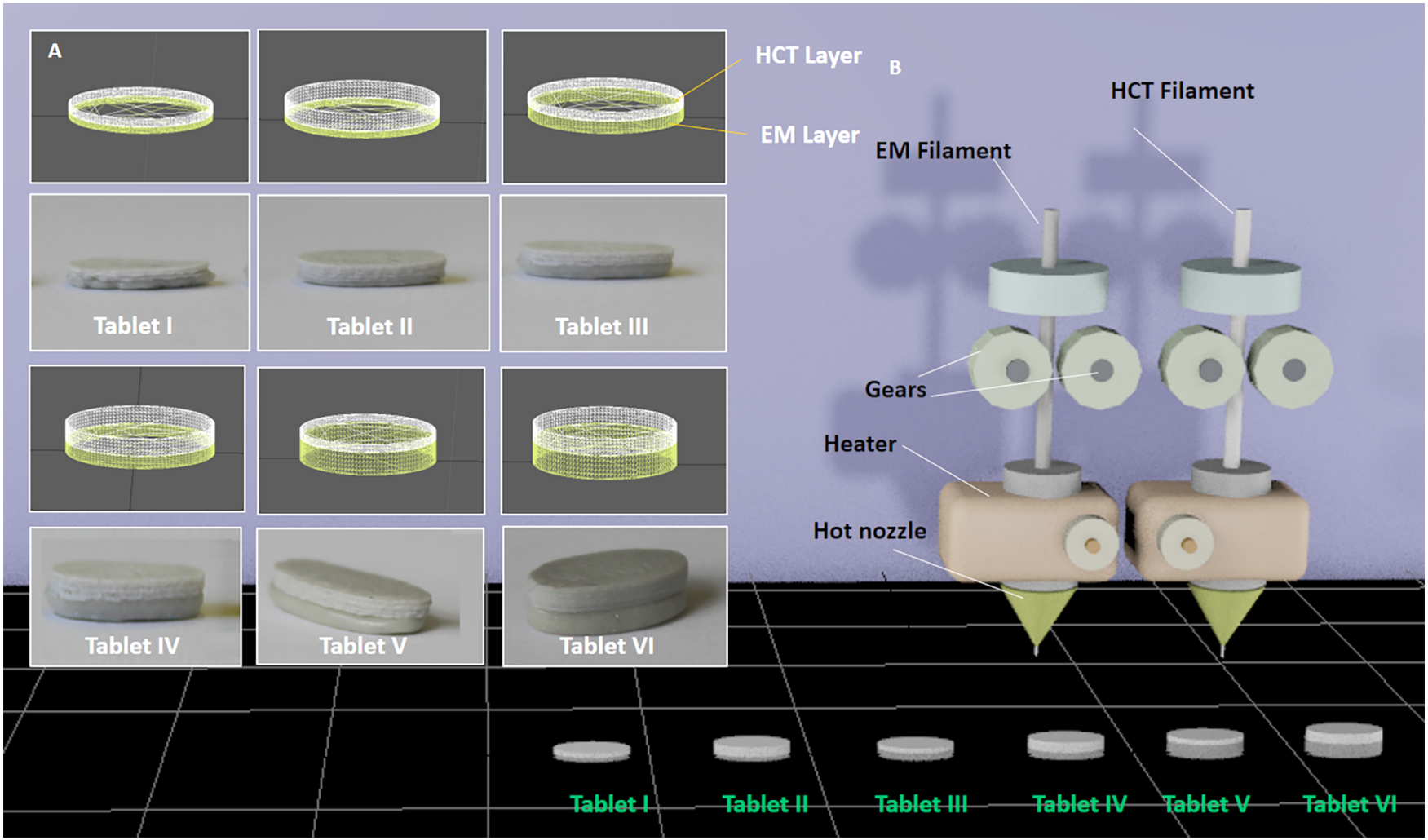

Fig. 1. (A) Rendered images (Autodesk 3DS Max) of bi-layered designs with unique dosage combination of EM and HCT, **(B)** Schematic diagram of dual 3D printer with EM and HCT loaded filament deployed in individual nozzles. The tablet were composed of lower EM layer and an upper HCT layer of variable volume to achieve different doses.

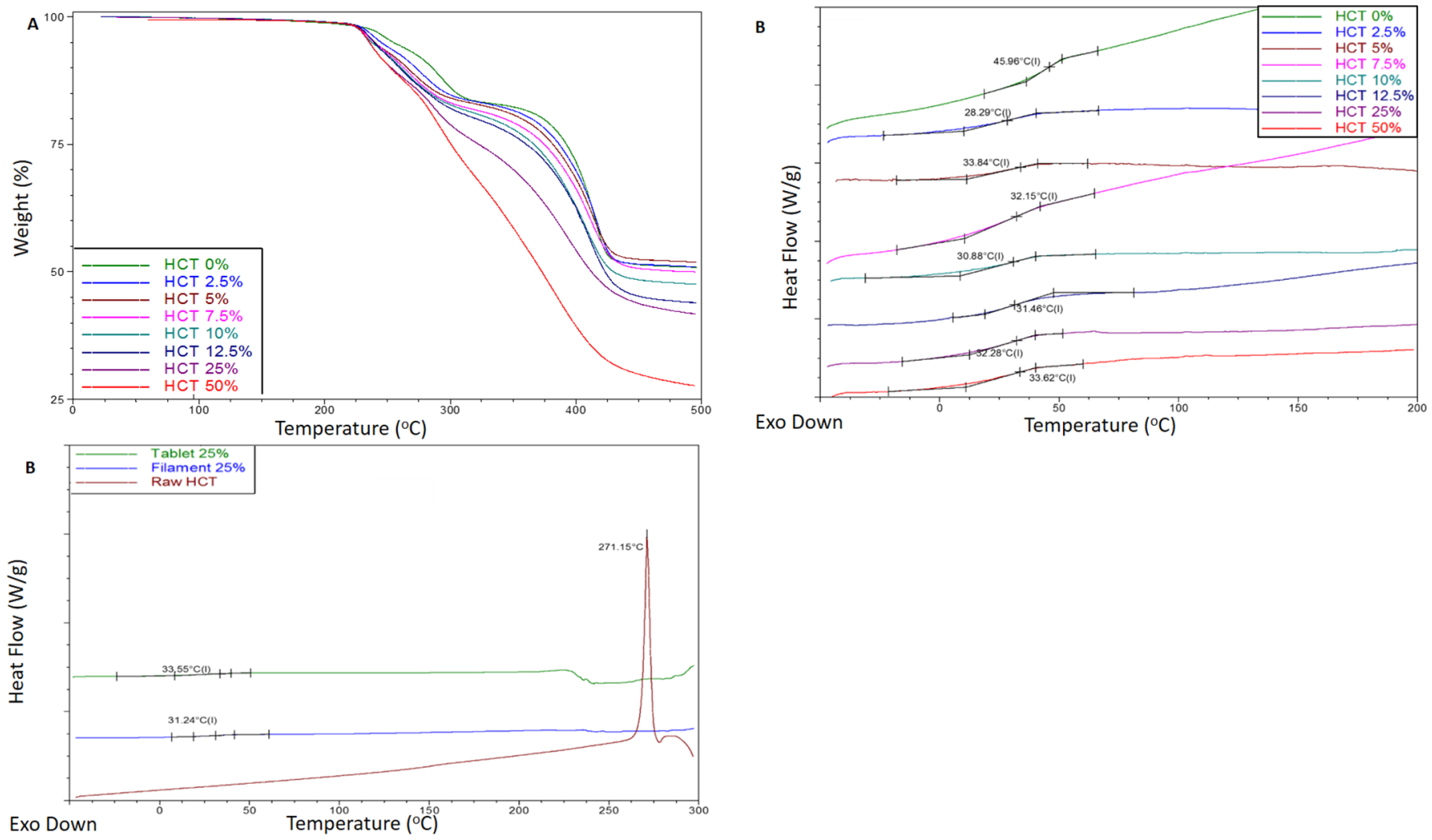

Fig. 2. (A)TGA thermal degradation profiles and **(b)** DSC thermographs of HCT loaded filament with HCT 0,2.5, 5, 7.5, 10, 12.5, 25 or 50%, of Eudragit EPO, HCT and (C) DSC thermographs of Eudragit EPO, HCT and drug loaded filament.

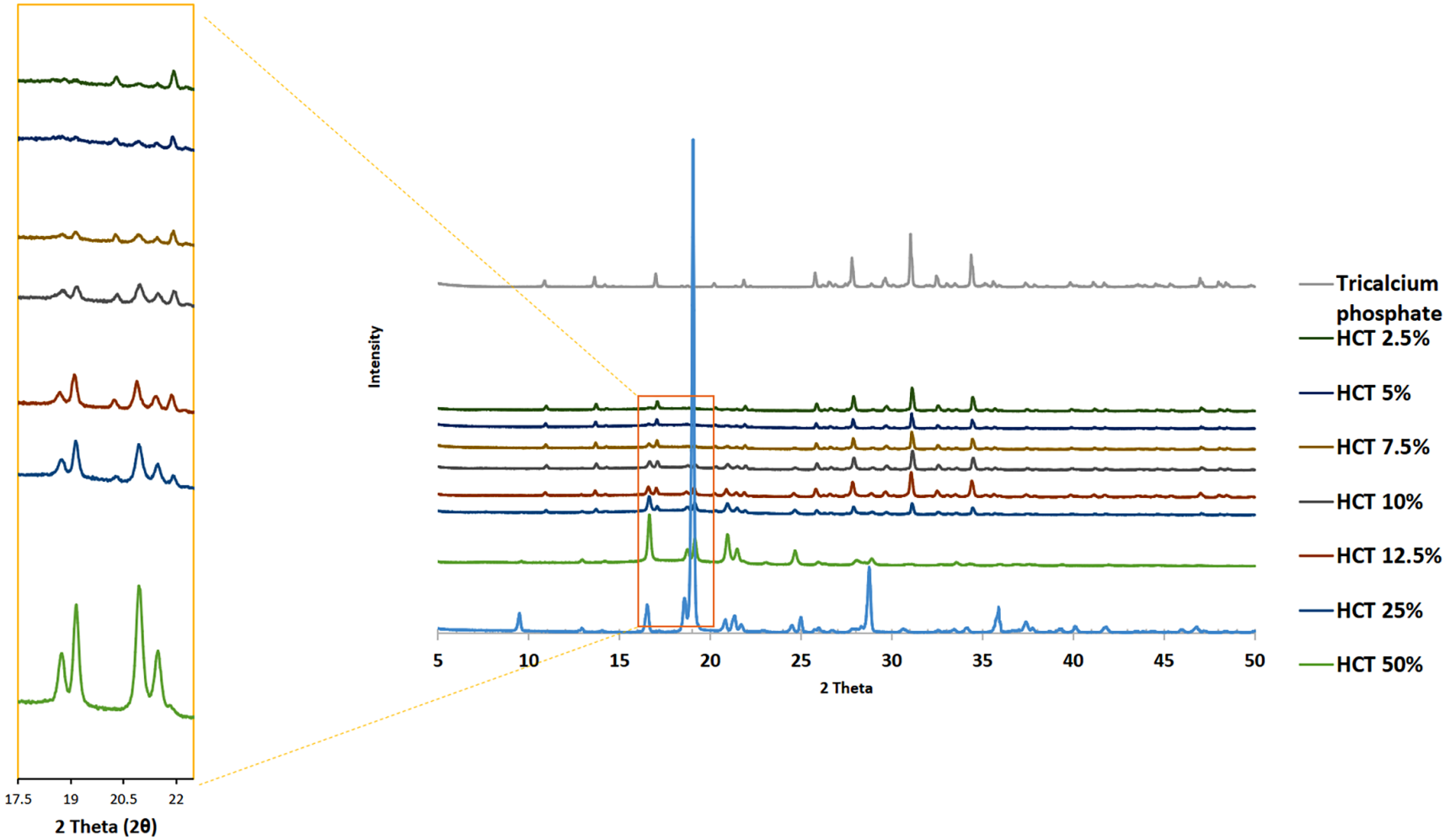

Fig. 3. XRD patterns of HCT loaded filament with HCT 0,2.5, 5, 7.5, 10, 12.5, 25 or 50%,

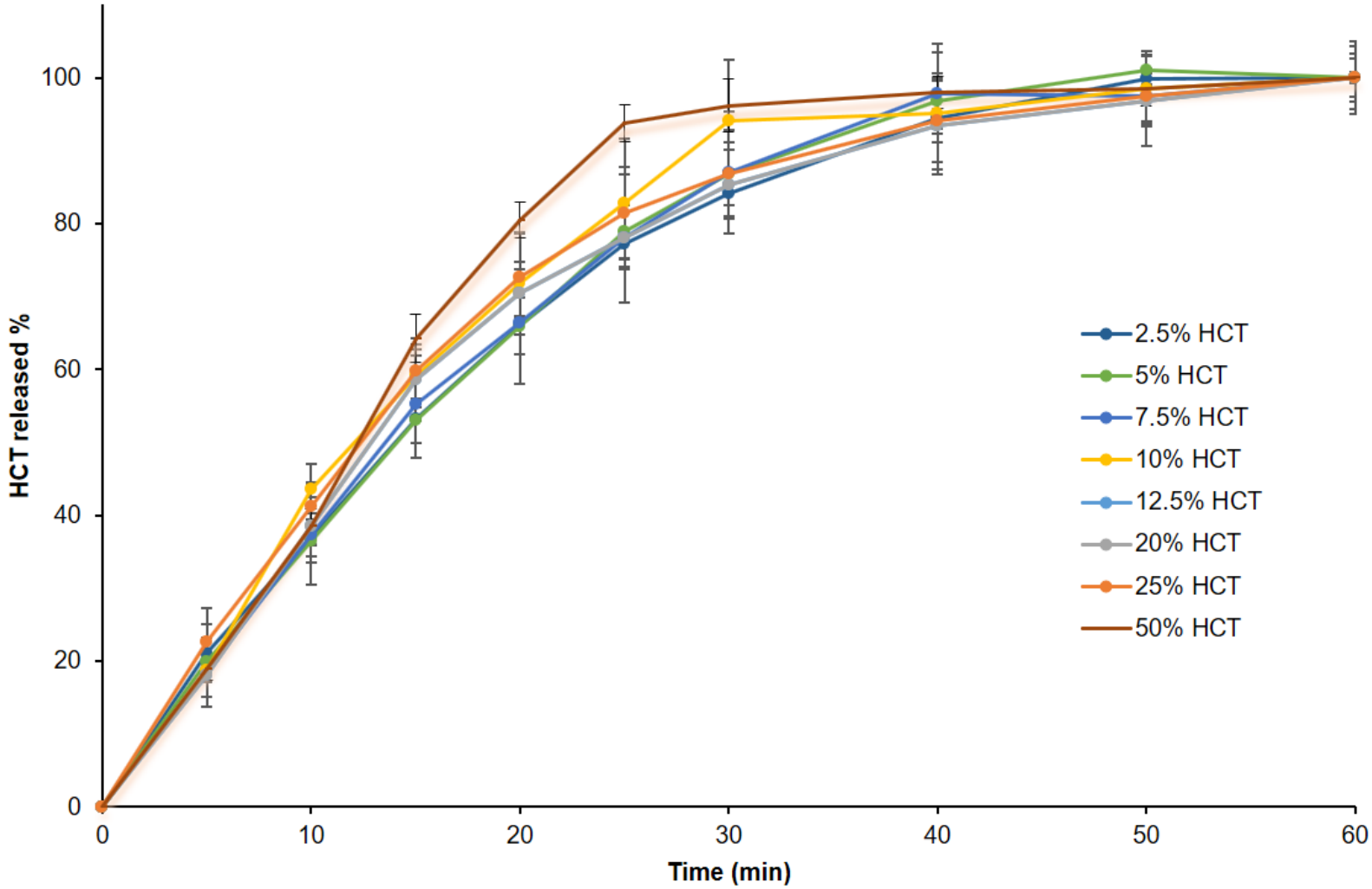

Fig. 4. *In vitro* release pattern of 3D printed tablets produced from HCT filament with HCT loading of 0,2.5, 5, 7.5, 10, 12.5, 25 or 50%,

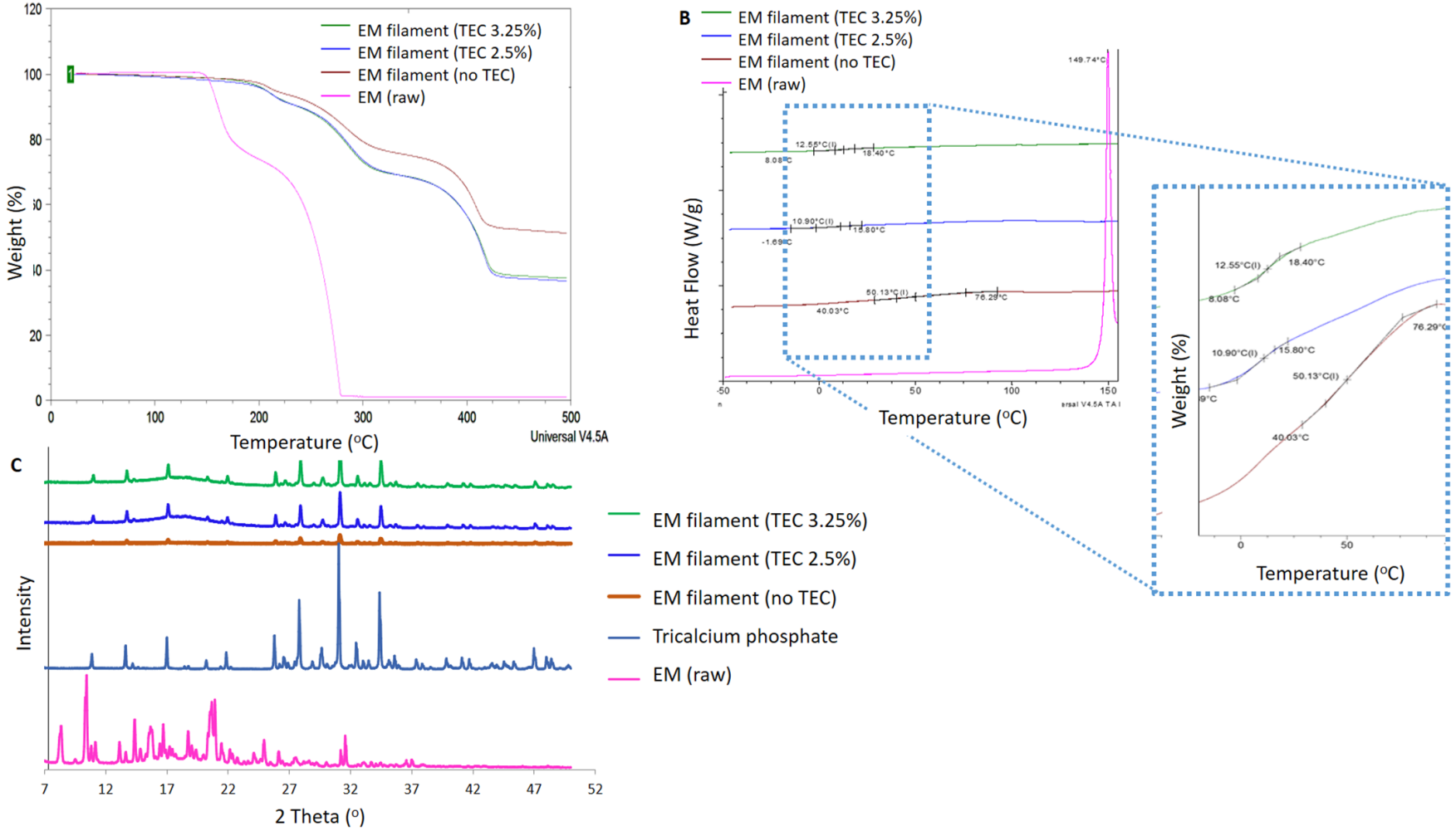

Fig. 5. A) TGA thermal degradation profiles, **(b)** DSC thermographs and **(C)** XRD patterns of EM and EM loaded filament with different levels of plasticiser (TEC 0, 2.5, 3.25%).

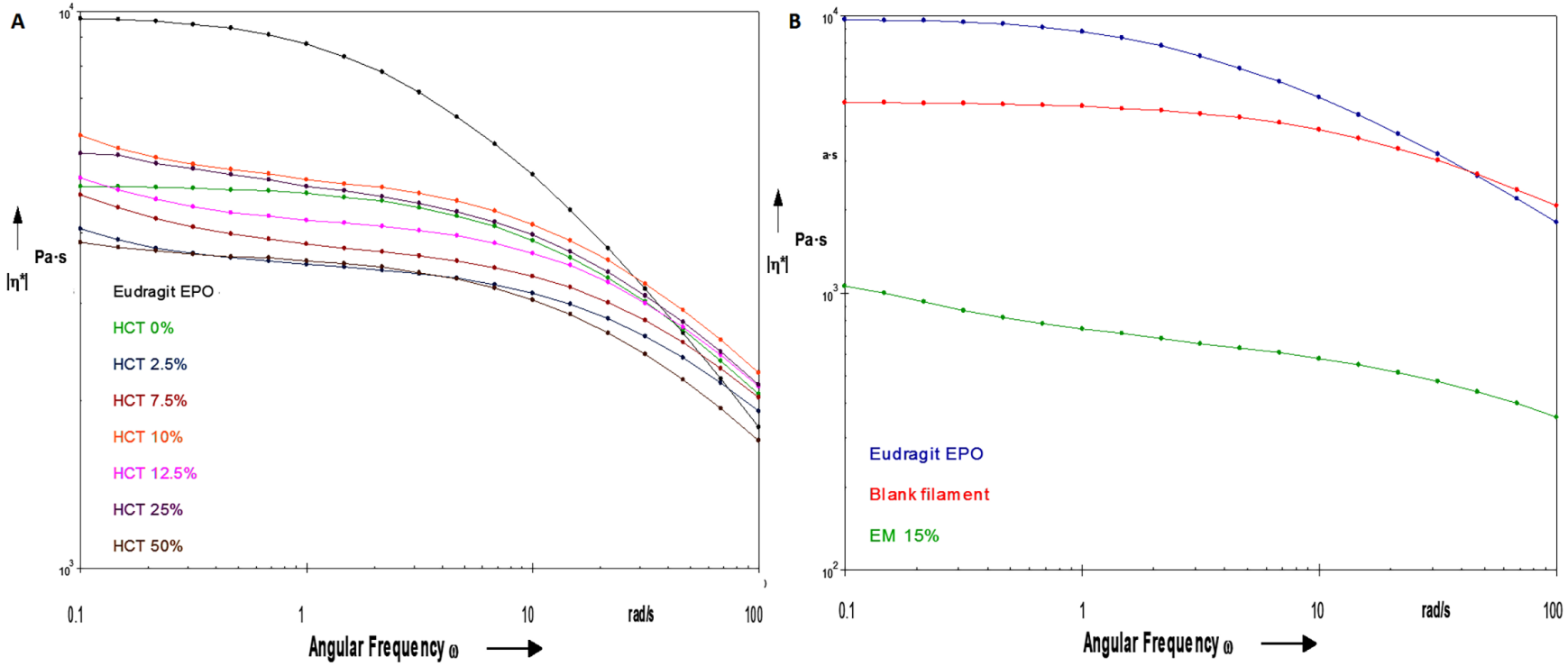

Fig. 6. Complex viscosity of Eudragit EPO and Eudragit EPO based filaments with (A) different HCT loadings and (B) EM as a function of the strain (T = 135 ^{o}C, v = 10 rad/sec).

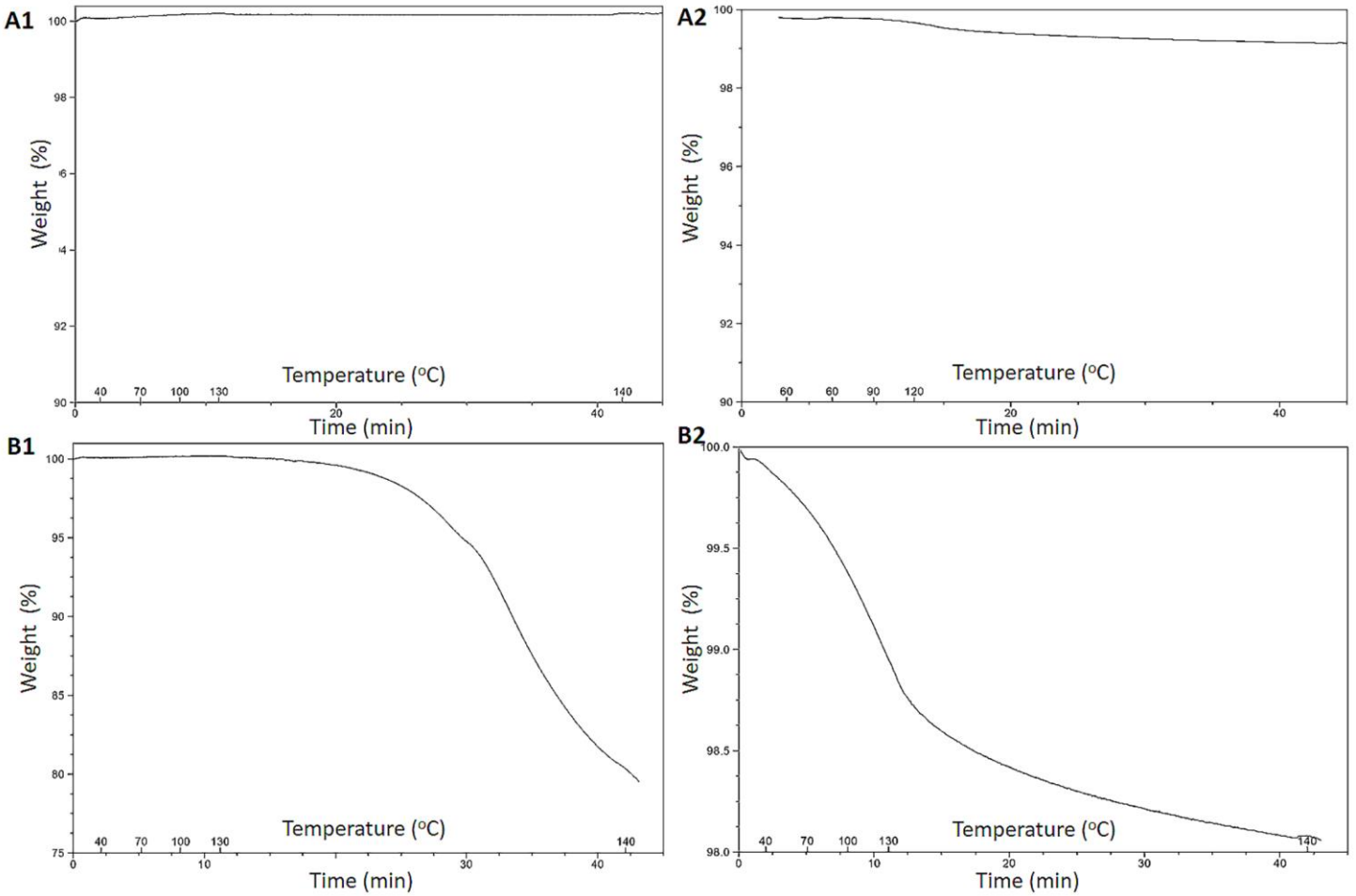

Fig. 7. TGA thermograph (isotherm for 30 min) at 135 °C for drug (as received) and filament under prolonged temperature for HCT **(A1,A2)** and EM **(B1, B2).**

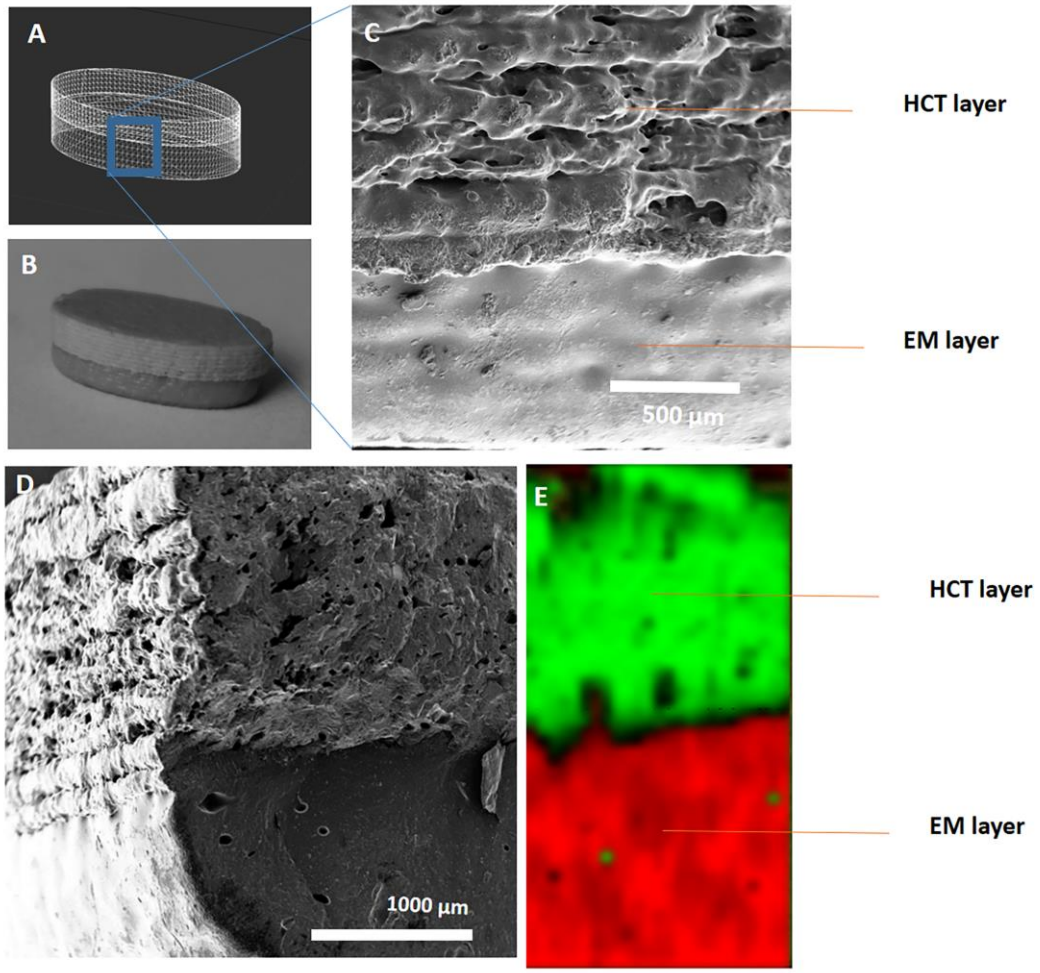

Fig. 8. (A) Rendered image and **(B)** photograph on 3D printed bi-layer tablets (composed of lower EM layer and an upper HCT layer), SEM image of **(C)** external surface and **(D)** cross section of bilayer tablets. Raman imaging of a cross section of bi-layer tablet (green =HCT, red=EM).

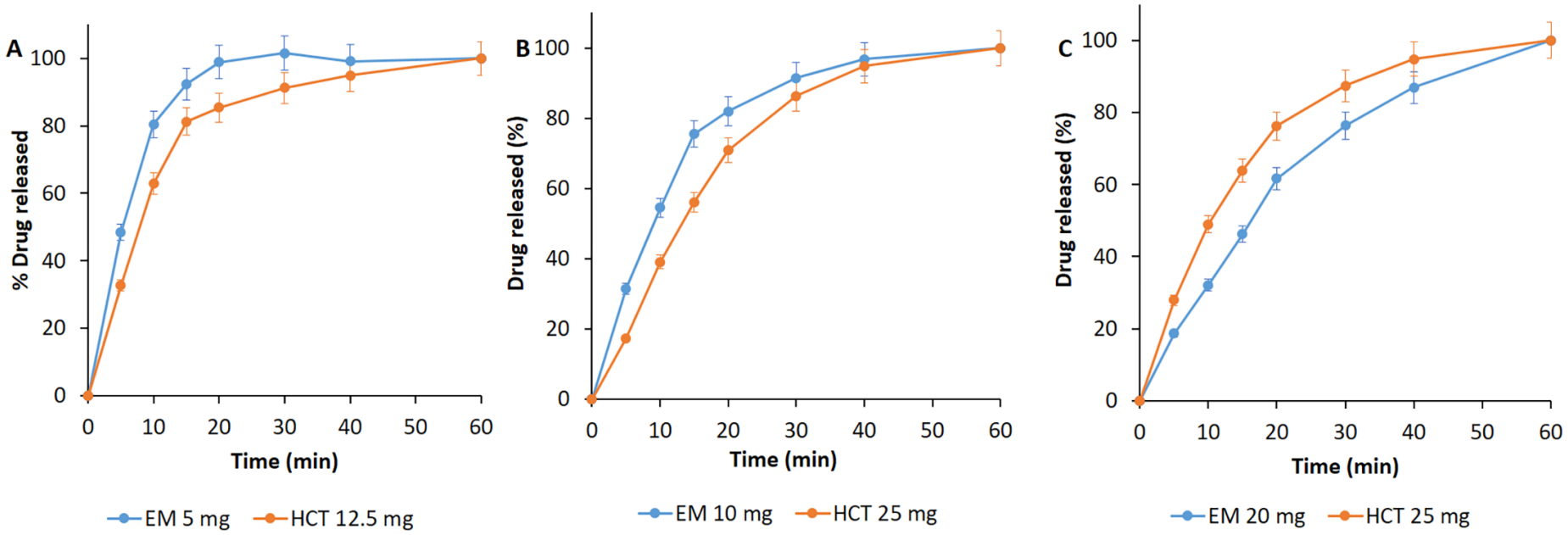

Fig. 9. *In vitro* drug release patterns for bilayer tablets of HCT and EM with distinct doses (a) 5mg: 12.5mg, (b) 10mg: 25mg, and 20mg: 25mg. (n=6, error bar =standard deviation).

From ‘fixed dose combinations’ to ‘a dynamic dose combiner’: 3D printed bi-layer antihypertensive tablets.

Muzna Sadia[1], Abdullah Isreb[1], Ibrahim Abbadi[1], Mohammad Isreb[2], David Aziz[1], Amjad Selo[3], Peter Timmins[4], Mohamed A Alhnan[1]*

Supplementary data

[1] School of Pharmacy and Biomedical Sciences, University of Central Lancashire, Preston, Lancashire, UK

[2]School of Pharmacy, University of Bradford, Richmond Road, Bradford, UK

[3]School of Pharmacy, University of Nottingham, Nottingham, UK

[4] Department of Pharmacy, University of Huddersfield, Huddersfield, UK

*Corresponding author: MAlbedAlhnan@uclan.ac.uk

University of Central Lancashire, MB025 Maudland Building, Preston PR1 2HE, UK

Tel: +44 (0)1772 893590, Fax: +44 (0)1772 892929

Table S1 Accuracy, reproducibility, limit of detection and limit of quantification of EM and HCT solution.

EM solution			**HCT solution**		
Accuracy			**Accuracy**		
Theoretical Concentration (mg/L)	Actual Concentration (mg/L) ±SD	Accuracy % ±SD	Measured Concentration (mg/L)	Calculated Concentration (mg/L) ±SD	Accuracy % ±SD
1.88	2.08±0.67	110.77±35.76	1.88	1.84±0.14	98.27±7.67
3.13	3.87±0.13	123.99±4.07	3.13	3.42±0.19	109.55±5.98
6.25	6.69±0.21	107.03±3.38	6.25	6.27±0.41	100.35±6.53
12.50	12.65±0.45	101.18±3.59	12.50	12.51±0.75	100.08±6.03
18.75	18.64±0.63	99.43±3.35	18.75	18.69±1.24	99.68±6.62
25	24.79±0.83	99.15±3.32	25.00	25.00±1.62	100±6.47
Repeatability			**Repeatability**		
25 mg/L	0.16%		25 mg/L	0.38%	
Limit of detection (LOD)*			**Limit of detection (LOD)**		
2.1 mg/L			0.5 mg/L		
Limit of quantification (LOQ)*			**Limit of quantification (LOQ)**		
6.87 mg/L			1.7 mg/L		

Limit of detection (LOD) and Limit of quantification (LOQ) was calculated as LOD = 3.3 σ/S and LOQ = 10 σ/S where σ is the residual standard deviation of the regression line and S is the slope of the calibration curve as per ICH-Q2 (R1) guidelines.

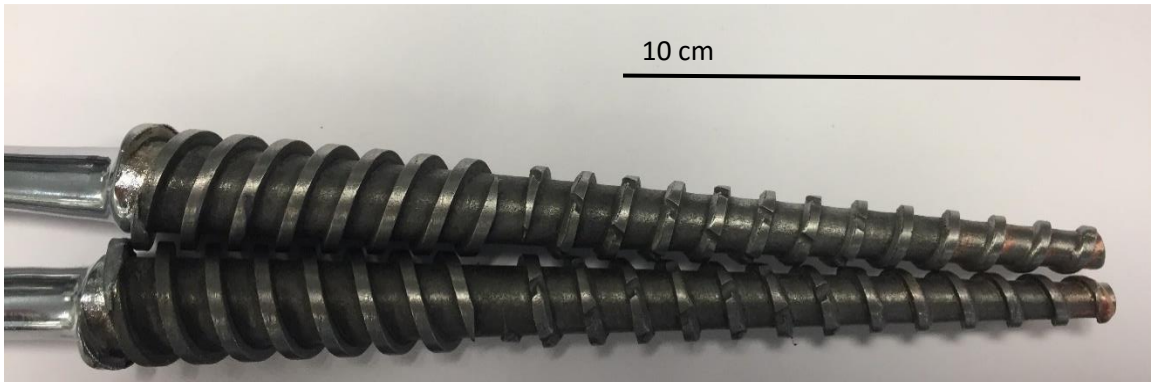

Fig S1 Photo for standard counter-rotating conical twin-screws used to equip a HAAKE MiniCTW benchtop hot-melt extruder (Thermo Scientific, Karlsruhe, Germany).

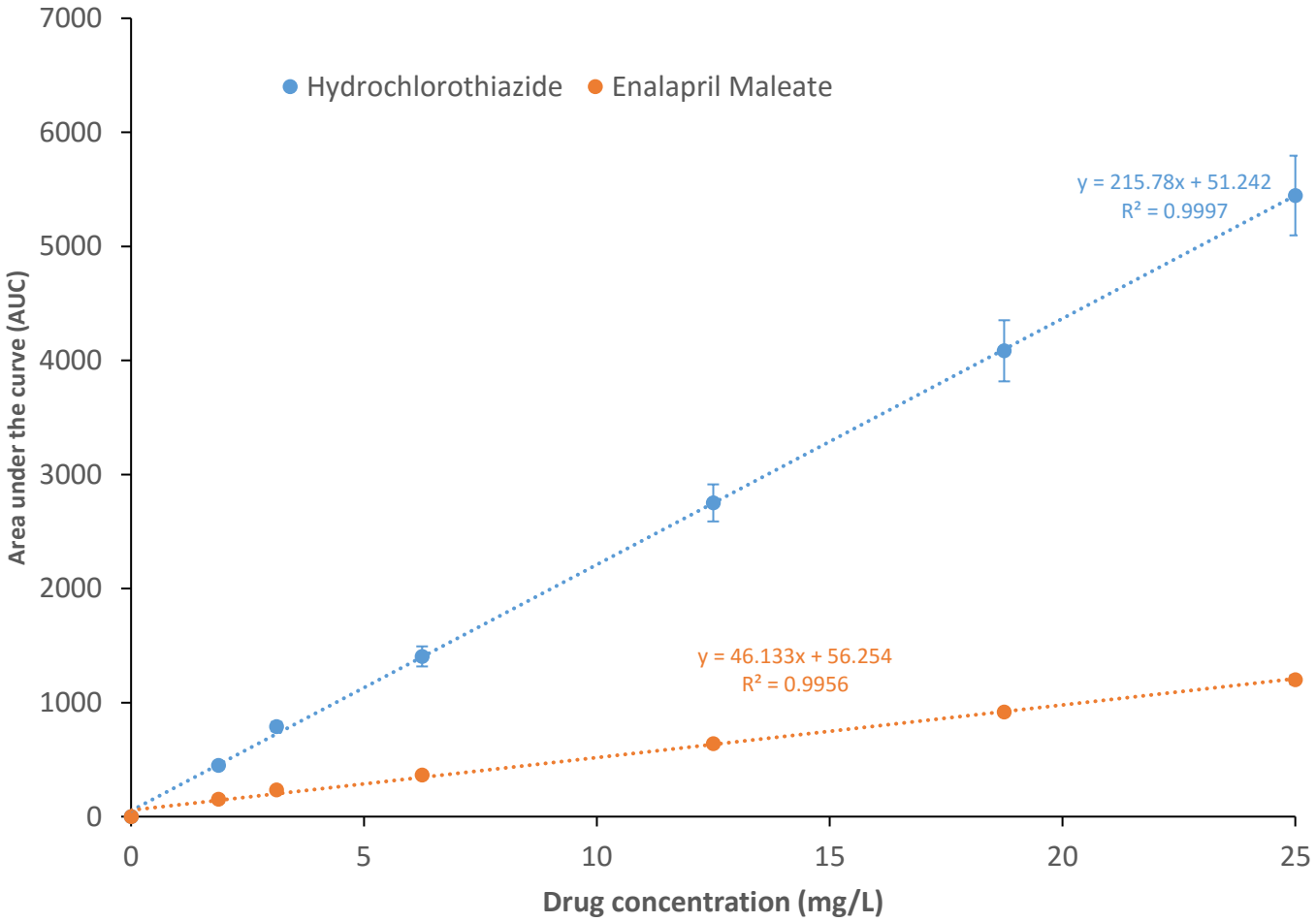

Fig S2 Standard linear curve of EM and HCT in pH 1.2 dissolution medium.

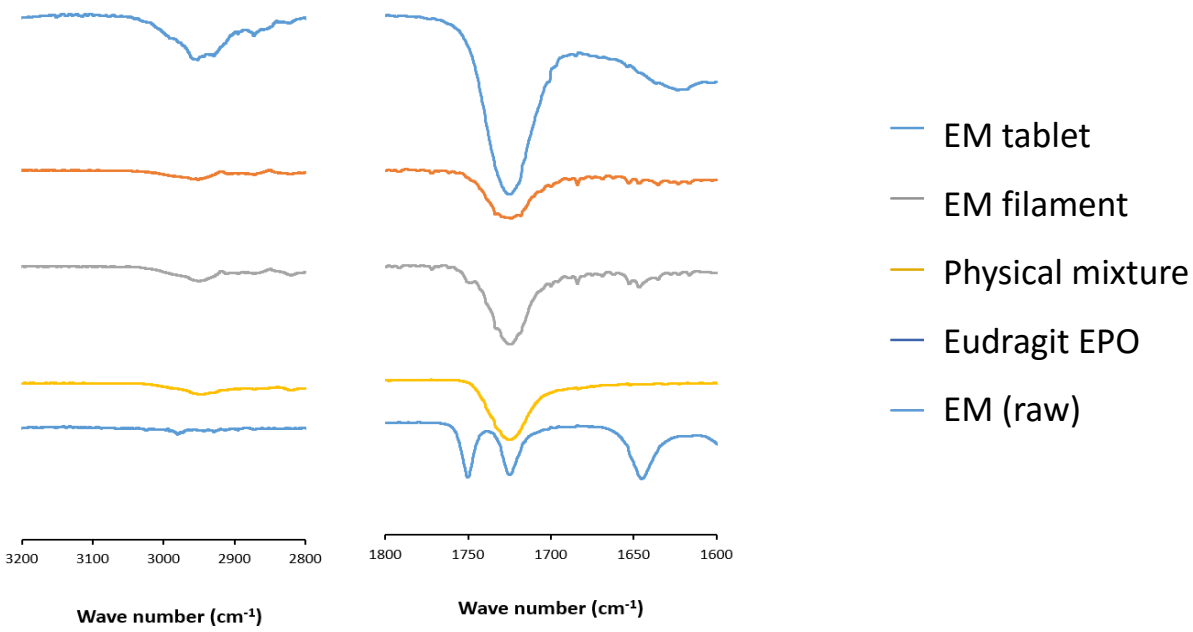

Fig S3 FTIR spectra of EM, Eudragit EPO, EM: Eudragit EPO physical mixture, EM loaded filament and tablet.

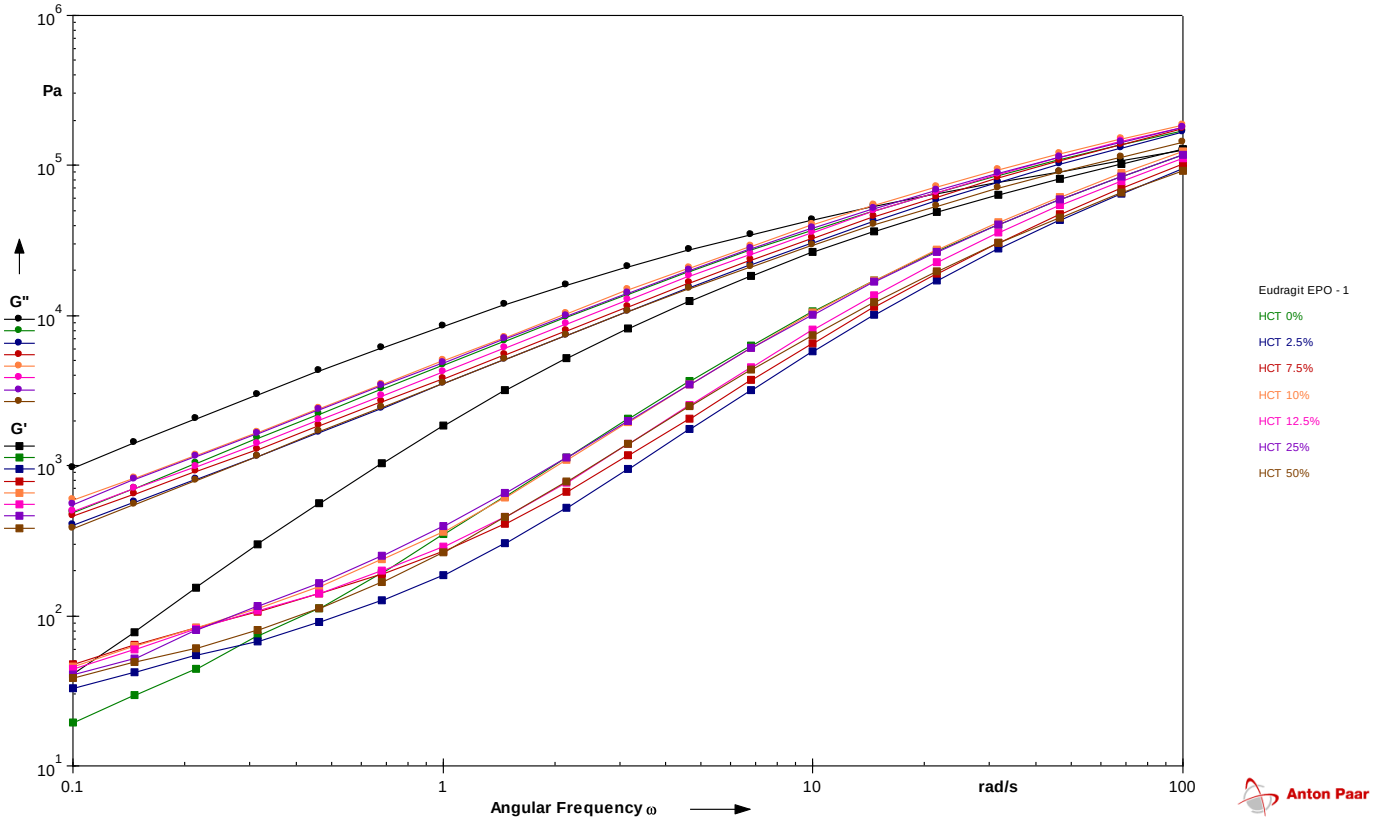

Fig S4 Storage (G') and loss (G") moduli of Eudragit EPO and polymeric filaments with different HCT loadings as a function of the strain (T = 135 ºC, v = 10 rad/sec).

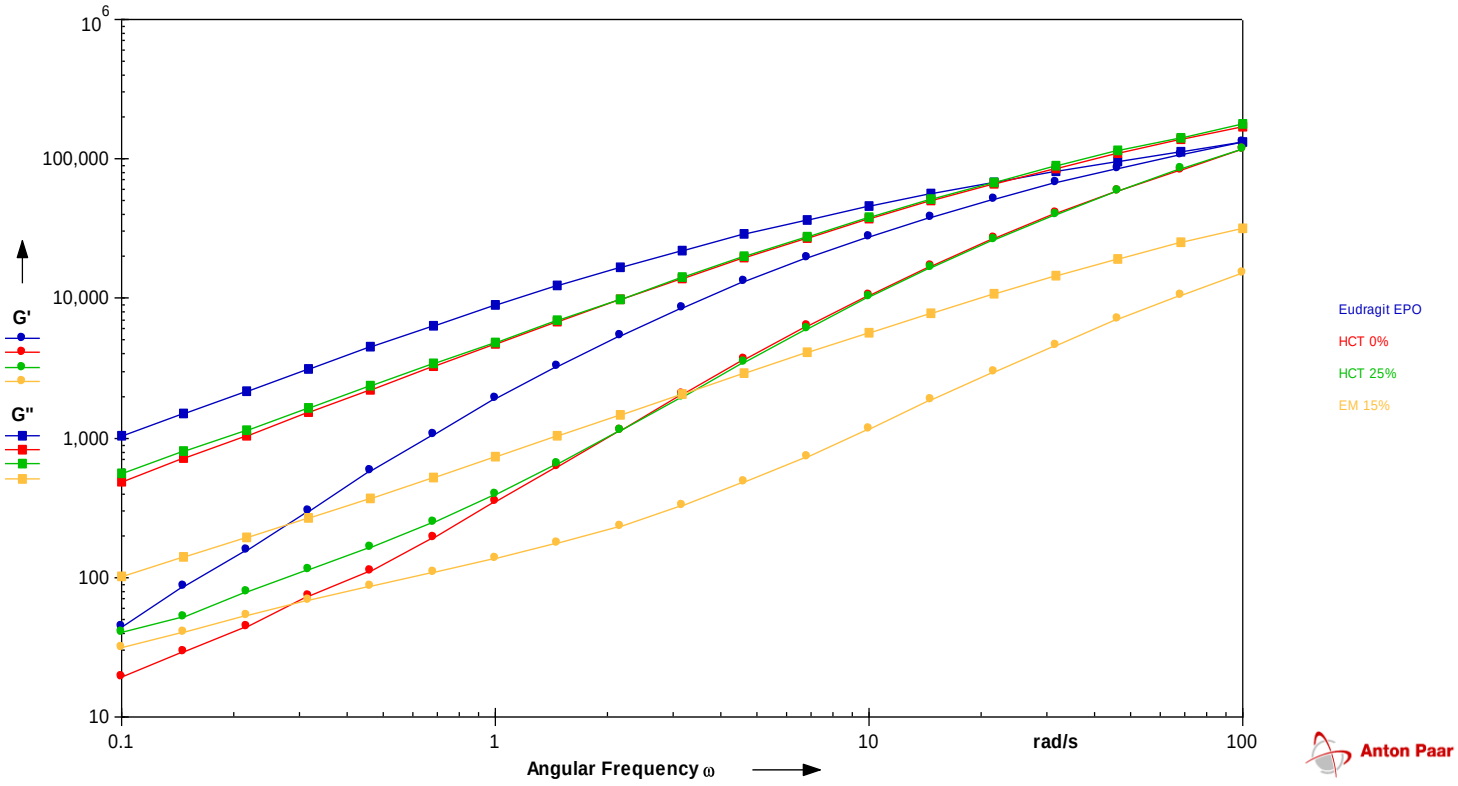

Fig S5 Storage (G') and loss (G") moduli of Eudragit EPO, blank and HCT and EM loaded Eudragit EPO based filaments as a function of the strain (T = 135 ^{o}C, v = 10 rad/sec).